Array Calibration in the Presence of Multipath

Amir Leshem, *Member, IEEE,* and Mati Wax, *Fellow, IEEE*

Abstract—We present an algorithm for the calibration of sensor arrays in the presence of multipath. The algorithm is based on two sets of calibration data obtained from two angularly separated transmitting points. We show the similarity between the calibration problem and blind identification of SIMO systems and analyze the identifiability of the problem. Simulation results demonstrating the performance of the algorithm are included.

Index Terms—Array calibration, blind channel identification, DOA estimation, multipath.

I. INTRODUCTION

MODERN super-resolution direction finding techniques such as minimum variance [1], MUSIC [4], subspace fitting methods [8], and maximum likelihood [12] presume the knowledge of the array response.

As the analysis of these techniques show [6], [7], [11], any inaccuracy in the presumed array response results in severe degradation of performance. The measurement of the array response, which is referred to as array calibration, is therefore a crucial step in the implementation of these techniques.

The existing calibration techniques [5], [9] are based on modeling the array response by a free-space model perturbed by an unknown coupling matrix and sensor location uncertainty. These unknown parameters are estimated together with the unknown signal parameters, assuming known or unknown source location. Yet, for general arrays with arbitrary sensor responses, these methods are no longer adequate since these modeling assumptions are no longer valid.

In this paper, we address the problem of measuring the array response of arrays with arbitrary sensor response in the presence of multipath. This problem is important since multipath is essentially unavoidable in practice, and it sets the limit on the achievable calibration accuracy.

The organization of the paper is as follows. In Section II, we formulate the problem. In Section III, we present the proposed solution. In Section VI, we present simulation results demonstrating the performance of the algorithm. Finally, in Section VII, we present some concluding remarks. In Section V, we consider the similarity and the differences between the calibration problem as presented here as well as the problem of blind identification of multiple FIR channels.
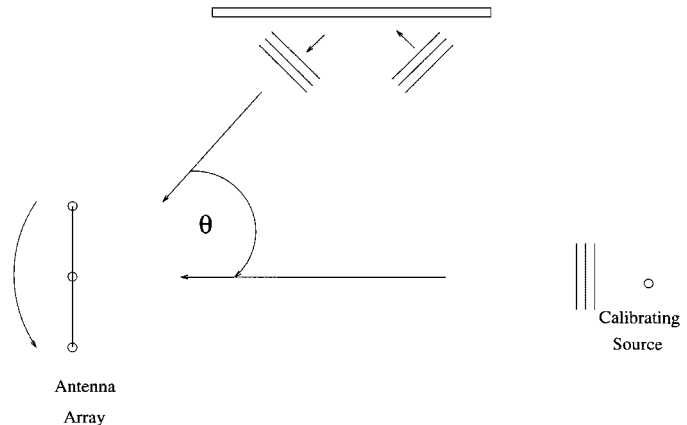
Fig. 1. Calibration setup (with one reflection).

II. PROBLEM FORMULATION

Let $\boldsymbol{a}(\theta)$ denote the $p \times 1$ vector of the array response to a source impinging from direction θ. The array calibration problem amounts to measuring $\boldsymbol{a}(\theta)$ for $\theta \in [0, 2\pi)$. It is usually performed by transmitting a signal from some location, rotating the array, and measuring the array response at each angle. Unfortunately, in many cases, the measured response is composed not only of the direct path from the transmitting point but also of multiple reflections from the surroundings; see Fig. 1. In the case of arbitrary array response, we can no longer resolve the multipath from a single set of measurements since the measured data can be considered to be the "true" array manifold. This situation is similar to the problem of blind identification of SIMO systems, wherein without any *a priori* knowledge of the signal, a single channel is not identifiable, and two channels are identifiable, even using second-order statistics only.

To cope with the multipath problem, we propose to carry out the calibration twice, i.e., rotate the array and measure the received array vector as a function of θ, yet each time use a different transmitting point. Let $\boldsymbol{y}_l(\theta)$ denote the $p \times 1$ vector received at the angle θ from the lth transmitting point ($l = 1, 2$). Assuming that the reflections are considered as point sources and all multipath effects are completely coherent with calibrating signals, i.e., each path differs by a complex reflection coefficient from the direct path, we get

$$\boldsymbol{y}_l(\theta) = \rho_{1,l}\boldsymbol{a}(\theta + \theta_{1,l}) + \sum_{i=2}^{r_l} \rho_{i,l}\boldsymbol{a}(\theta + \theta_{i,l}) + \boldsymbol{n}_l(\theta)$$
$$l = 1, 2 \tag{1}$$

where

$\theta_{i,l}$　　direction of the ith reflection in the lth set;

$\rho_{i,l}$ complex coefficient representing the phase shift and the amplitude of the ith reflection in the lth set;

r_l number of reflections in the lth set;

$\boldsymbol{n}_l(\theta)$ noise vector for the angle θ in the lth set.

Since the array manifold is measured relative to some arbitrary point and the relative angle between the measurement points is known, we can assume without loss of generality that $\rho_{1,1} = 1$ and $\theta_{1,1} = \theta_{1,2} = 0°$. In addition, since the reflecting objects remain fixed while the transmitting point change, the relative directions of the reflections are different, i.e., $\boldsymbol{\theta}_{i,1} \neq \boldsymbol{\theta}_{i,2}$ ($i \neq 1$).

Assuming that the calibration process consists of N measurements taken uniformly on $\theta \in [0, 2\pi)$, it follows from (1) that the measured data is given by

$$\boldsymbol{y}_l\left(\frac{2\pi k}{N}\right) = \sum_{i=1}^{r_l} \rho_{i,l}\boldsymbol{a}\left(\frac{2\pi k}{N} + \theta_{i,l}\right) + \boldsymbol{n}_l(k)$$
$$l = 1, 2; \ k = 0, \cdots, N - 1 \qquad (2)$$

where we use $\boldsymbol{n}_l(k)$ to emphasize that the noise is not angle dependent. Note that we have included the direct path with the multipath.

In our solution, we make the following assumption:

A1) All reflections $\theta_{i,l}$ are a multiple of the basic rotation $2\pi/N$.

Assumption A1) serves as a very good approximation when the grid is fine.

The array calibration problem can now be formulated as follows. Given the two measured data sets

$$\left\{\boldsymbol{y}_l\left(\frac{2\pi k}{N}\right)\right\}_{k=0}^{N-1} \qquad (l = 1, 2)$$

estimate the array manifold

$$\left\{\boldsymbol{a}\left(\frac{2\pi k}{N}\right)\right\}_{k=0}^{N-1}.$$

III. THE MAXIMUM LIKELIHOOD ESTIMATOR

The proposed solution is based on two steps:

 i) estimating the reflections' parameters $\{\boldsymbol{\rho}_l, \boldsymbol{\theta}_l\}$;

 ii) estimating the array manifold using the estimated reflections;

where $\boldsymbol{\rho}_l = [\rho_{1,l}, \cdots, \rho_{r_l,l}]$ is the vector of the reflection coefficients at the lth set of measurements, and $\boldsymbol{\theta}_l = [\theta_{1,l}, \cdots, \theta_{r_l,l}]$ is the vector of the reflections' DOA's at the lth set of measurements.

For the first step, we have two approaches. The first approach uses the LS estimator, which is identical to the MLE under the assumption of white Gaussian noise. This estimator is derived in this section. The second approach uses a simplified LS, which we derive in the next section.

The second step is derived by a least squares solution, which is the MLE under the assumption of white Gaussian noise. This step is performed identically in the two approaches using the results of the first step.

To carry out the derivation of the MLE, let $\boldsymbol{w}_l$ denote the $N \times 1$ vector whose kth element is $\rho_{i,l}$ if $2\pi k/N = \theta_{i,l}$ and zero otherwise. Mathematically, this is expressed as

$$w_l(k) = \sum_{i=1}^{r_l} \rho_{i,l}\delta\left(\frac{2\pi k}{N} - \theta_{i,l}\right) \qquad (3)$$

where $\delta(\theta)$ is the delta function. Let $\boldsymbol{a}_m$ be the $N \times 1$ array manifold of the mth sensor

$$\boldsymbol{a}_m = \left[a_m(0), a_m\left(\frac{2\pi}{N}\right), \cdots, a_m\left(\frac{2\pi(N-1)}{N}\right)\right]^T \quad (4)$$
$$\boldsymbol{y}_{m,l} = [y_{m,l}(1), \cdots, y_{m,l}(N)]^T \qquad (5)$$
$$\boldsymbol{n}_{m,l} = [n_{m,l}(1), \cdots, n_{m,l}(N)]^T \qquad (6)$$

and $y_{m,l}(k)$ and $n_{m,l}(k)$ are the mth element of $\boldsymbol{y}_l(2\pi k/N)$ and $\boldsymbol{n}_l(k)$, respectively.

With this notation, we can rewrite (2) as

$$\begin{aligned}\boldsymbol{y}_{m,l} &= \sum_{i=1}^{r_l} \rho_{i,l}(\boldsymbol{P}_{k_{i,l}})\boldsymbol{a}_m + \boldsymbol{n}_l \\ &= \sum_{i=1}^{r_l} w_l(k_{i,l})\boldsymbol{P}_{k_{i,l}}\boldsymbol{a}_m + \boldsymbol{n}_l \\ &= \left[\sum_{i=1}^{r_l} w_l(k_{i,l})\boldsymbol{P}_{k_{i,l}}\right]\boldsymbol{a}_m + \boldsymbol{n}_l \\ &= \left[\sum_{k=0}^{N-1} w_l(k)\boldsymbol{P}_k\right]\boldsymbol{a}_m + \boldsymbol{n}_l \qquad (7)\end{aligned}$$

where $k_{i,l} = (\theta_{i,l}/(2\pi/N))$, and $\boldsymbol{P}_k$ is a permutation matrix that rotates the zeroth element of $\boldsymbol{a}$ into the kth position defined by

$$(\boldsymbol{P}_k)_{m,n} = \begin{cases} 1, & \text{if } m + k = n \text{ or } m + k - N = n \\ 0, & \text{otherwise.} \end{cases} \qquad (8)$$

The last equality in (7) is due to the fact the $w(k) = 0$ if $\nexists i$ such that $2\pi k/N = \theta_{i,l}$. Denoting

$$\boldsymbol{A}_l = \sum_{k=0}^{N-1} w_l(k)\boldsymbol{P}_k \qquad (9)$$

it follows that $\boldsymbol{A}_l$ is an $N \times N$ circulant matrix generated by $\boldsymbol{w}_l$

$$\boldsymbol{A}_l = \begin{bmatrix} w_l(0) & \cdots & w_l(N-2) & w_l(N-1) \\ w_l(N-1) & w_l(0) & \cdots & w_l(N-2) \\ \vdots & & & \vdots \\ w_l(1) & \cdots & w_l(N-1) & w_l(0) \end{bmatrix}. \qquad (10)$$

Thus, we can rewrite (2) as

$$\boldsymbol{y}_{m,l} = \boldsymbol{A}_l\boldsymbol{a}_m + \boldsymbol{n}_{m,l} \qquad 1 \leq m \leq p. \qquad (11)$$

Since $\boldsymbol{A}_l$ is a circulant matrix, it is diagonalized by the DFT matrix of order N, and its eigenvalues are given by the DFT of the generating vector $\boldsymbol{w}_l$ [2]. Therefore

$$\boldsymbol{F}^H \boldsymbol{A}_l \boldsymbol{F} = \text{diag}\{\boldsymbol{F}\boldsymbol{w}_l\} = \text{diag}\{\hat{\boldsymbol{w}}_l\} \qquad (12)$$

where F is the normalized DFT matrix of order N ($FF^H = I$), and $\hat{w}_l = Fw_l$ is the DFT of w_l given by

$$\hat{w}_l(k) = \frac{1}{\sqrt{N}} \sum_{i=1}^{r_1} \rho_{i,l} e^{-j(2\pi k/N)k_{i,l}}. \tag{13}$$

Hence

$$A_l = F \operatorname{diag}\{\hat{w}_l\} F^H. \tag{14}$$

With this representation of the matrices A_l, we can derive a somewhat simplified expression of the MLE.

Let

$$y_m = \begin{bmatrix} y_{m,1} \\ y_{m,2} \end{bmatrix} \quad \text{and} \quad A = \begin{bmatrix} A_1 \\ A_2 \end{bmatrix}.$$

Assuming that the noise is white and Gaussian from (11), the MLE is given by

$$\left[\tilde{a}_1, \cdots, \tilde{a}_p, \tilde{\theta}_1, \tilde{\theta}_2, \tilde{\rho}_1, \tilde{\rho}_2\right]$$
$$= \arg \min_{a_1, \cdots, a_p, \theta_1, \theta_2, \rho_1, \rho_2} \sum_{m=1}^{p} \|y_m - A a_m\|^2. \tag{15}$$

Minimizing first with respect to a_m, we obtain

$$\tilde{a}_m = \left(A^H A\right)^{-1} A^H y_m. \tag{16}$$

Now, from the definition of A and (14), we obtain

$$A^H A = F \left(\left|\hat{W}_1\right|^2 + \left|\hat{W}_2\right|^2\right) F^H \tag{17}$$

where $\hat{W}_l = \operatorname{diag}(Fw_l)$. Substituting (14) and (17) into (16) yields

$$\tilde{a}_m = FD \left(\hat{W}_1^H \check{y}_{m,1} + \hat{W}_2^H \check{y}_{m,2}\right) \tag{18}$$

where

$$D = \left(\left|\hat{W}_1\right|^2 + \left|\hat{W}_2\right|^2\right)^{-1} \tag{19}$$

and $\check{y}_{m,l} = F^H y_{m,l}$. Finally, substituting (14) and (18) into (15), we obtain

$$\left[\tilde{\theta}_1, \tilde{\theta}_2, \tilde{\rho}_1, \tilde{\rho}_2\right]$$
$$= \arg \min_{\theta_1, \theta_2, \rho_1, \rho_2} \sum_{m=1}^{p} \sum_{l=1}^{2} \left\|y_{m,l} - F\hat{W}_l D \hat{W}_l^H F^H y_{m,l}\right\|^2 \tag{20}$$

which can also be rewritten as

$$\left[\tilde{\theta}_1, \tilde{\theta}_2, \tilde{\rho}_1, \tilde{\rho}_2\right]$$
$$= \arg \min_{\theta_1, \theta_2, \rho_1, \rho_2} \sum_{m=1}^{p} \sum_{l=1}^{2} \left\|\left(I - \hat{W}_l D \hat{W}_l^H\right) \check{y}_{m,l}\right\|^2. \tag{21}$$

Notice that this estimator involves all the reflections parameters, i.e., the DOA's and the reflection coefficients, in a highly nonlinear fashion and, hence, is computationally unattractive.

IV. SIMPLE LS ESTIMATOR

In this section, we derive a simplified LS estimator for the reflections DOA's and reflection coefficients. This estimator, together with the estimator for a_m given in (18), consists of the simplified LS estimator for the array manifold.

Substituting (14) into (11), we obtain

$$F^H a_m = \operatorname{diag}(\hat{w}_l)^{-1} (\check{y}_{m,l} - \check{n}_{m,l}) \tag{22}$$

where $\check{n}_{m,l} = F^H n_{m,l}$. Since this holds for both sets of measurements, we obtain

$$\hat{W}_1^{-1} (\check{y}_{m,1} - \check{n}_{m,1}) = \hat{W}_2^{-1} (\check{y}_{m,2} - \check{n}_{m,2}) \tag{23}$$

which can be rewritten as

$$\hat{w}_1 \circ \check{y}_{m,2} - \hat{w}_2 \circ \check{y}_{m,1} = \hat{w}_1 \circ \check{n}_{m,2} - \hat{w}_2 \circ \check{n}_{m,1} \tag{24}$$

where $\circ$ denotes elementwise multiplication.

Since the right-hand side of (24) is "noise," a possible LS estimator for the reflections' parameters is given by

$$\left[\tilde{\theta}_1, \tilde{\theta}_2, \tilde{\rho}_1, \tilde{\rho}_2\right] = \min_{\theta_1, \theta_2, \rho_1, \rho_2} \|\hat{w}_1 \circ \check{y}_{m,2} - \hat{w}_2 \circ \check{y}_{m,1}\|^2. \tag{25}$$

Substituting (13) into (25) yields

$$\left[\tilde{\theta}_1, \tilde{\theta}_2, \tilde{\rho}_1, \tilde{\rho}_2\right]$$
$$= \min_{\theta_1, \theta_2, \rho_1, \rho_2} \sum_{k=0}^{N-1} \left\| \check{y}_{m,2}(k) \sum_{i=1}^{r_1} \rho_{i,1} e^{-j(2\pi k/N)k_{i,1}} \right.$$
$$\left. - \check{y}_{m,1}(k) \sum_{i=1}^{r_2} \rho_{i,2} e^{-j(2\pi k/N)k_{i,2}} \right\|^2 \tag{26}$$

where $k_{i,l} = (\theta_{i,l}/(2\pi k/N))$. Denoting

$$\Upsilon_1(k, \theta) = \check{y}_{m,1}(k) e^{-jk\theta} \tag{27}$$
$$\Upsilon_2(k, \theta) = \check{y}_{m,2}(k) e^{-jk\theta} \tag{28}$$

and (29), shown at the bottom of the page, we can rewrite (26) as a linear problem in ρ (recall that we have assumed $\rho_{1,1} = 1$ and $\theta_{1,1} = 0°$)

$$\left[\tilde{\theta}_1, \tilde{\theta}_2, \tilde{\rho}\right] = \min_{\theta_1, \theta_2, \rho} \|B_m(\theta_1, \theta_2)\rho + \check{y}_{m,2}\|^2. \tag{30}$$

$$B_m = \begin{pmatrix} \Upsilon_2(0, \theta_{2,1}) & \cdots & \Upsilon_2(0, \theta_{r_1,1}) & -\Upsilon_1(0, \theta_{1,2}) & \cdots & -\Upsilon_1(0, \theta_{r_2,2}) \\ \vdots & & & & & \vdots \\ \Upsilon_2(N-1, \theta_{2,1}) & \cdots & \Upsilon_2(N-1, \theta_{r_1,1}) & -\Upsilon_1(N-1, \theta_{1,2}) & \cdots & -\Upsilon_1(N-1, \theta_{r_2,2}) \end{pmatrix}$$

$$\rho = [\rho_{2,1}, \cdots, \rho_{r_1,1}, \rho_{1,2}, \cdots, \rho_{r_2,2}]^T \tag{29}$$

This estimator is based on the data of the mth sensor only. Clearly, we can improve the performance by combining the information from all sensors. This yields

$$\left[\tilde{\boldsymbol{\theta}}_1, \tilde{\boldsymbol{\theta}}_2, \tilde{\boldsymbol{\rho}}\right] = \arg \min_{\boldsymbol{\theta}_1, \boldsymbol{\theta}_2, \boldsymbol{\rho}} \sum_{m=1}^{p} \|\boldsymbol{B}_m(\boldsymbol{\theta}_1, \boldsymbol{\theta}_2)\boldsymbol{\rho} + \check{\boldsymbol{y}}_{m,2}\|^2. \tag{31}$$

To evaluate this estimator, we first rewrite it in matrix form as

$$\left[\tilde{\boldsymbol{\theta}}_1, \tilde{\boldsymbol{\theta}}_2, \tilde{\boldsymbol{\rho}}\right] = \arg \min_{\boldsymbol{\theta}_1, \boldsymbol{\theta}_2, \boldsymbol{\rho}} \|\boldsymbol{B}(\boldsymbol{\theta}_1, \boldsymbol{\theta}_2)\boldsymbol{\rho} + \check{\boldsymbol{y}}_2\|^2 \tag{32}$$

where

$$\boldsymbol{B}(\boldsymbol{\theta}_1, \boldsymbol{\theta}_2) = \left[\boldsymbol{B}_1^T(\boldsymbol{\theta}_1, \boldsymbol{\theta}_2), \cdots, \boldsymbol{B}_m^T(\boldsymbol{\theta}_1, \boldsymbol{\theta}_2)\right]^T \tag{33}$$

and

$$\check{\boldsymbol{y}}_2 = \left[\check{\boldsymbol{y}}_{12}^T, \cdots, \check{\boldsymbol{y}}_{p2}^T\right]^T. \tag{34}$$

Minimizing first with respect to $\boldsymbol{\rho}$, with $\boldsymbol{\theta}_1, \boldsymbol{\theta}_2$ being fixed, we obtain the well-known least squares solution

$$\tilde{\boldsymbol{\rho}} = -\left(\boldsymbol{B}(\boldsymbol{\theta}_1, \boldsymbol{\theta}_2)^H \boldsymbol{B}(\boldsymbol{\theta}_1, \boldsymbol{\theta}_2)\right)^{-1} \boldsymbol{B}(\boldsymbol{\theta}_1, \boldsymbol{\theta}_2)^H \check{\boldsymbol{y}}_2. \tag{35}$$

Substituting (35) back into (32), the resulting estimator of the directions-of-arrival of the reflections is

$$\left[\tilde{\boldsymbol{\theta}}_1, \tilde{\boldsymbol{\theta}}_2\right] = \arg \min_{\boldsymbol{\theta}_1, \boldsymbol{\theta}_2} \left\|\boldsymbol{P}_{\boldsymbol{B}(\boldsymbol{\theta}_1, \boldsymbol{\theta}_2)}^{\perp}(\check{\boldsymbol{y}}_{m,2})\right\|^2 \tag{36}$$

where $\boldsymbol{P}_{\boldsymbol{B}(\boldsymbol{\theta}_1, \boldsymbol{\theta}_2)}^{\perp}$ is the projection on the orthogonal complement of the subspace spanned by the columns of $\boldsymbol{B}(\boldsymbol{\theta}_1, \boldsymbol{\theta}_2)$

$$\boldsymbol{P}_{\boldsymbol{B}(\boldsymbol{\theta}_1, \boldsymbol{\theta}_2)}^{\perp}$$
$$= \boldsymbol{I} - \boldsymbol{B}(\boldsymbol{\theta}_1, \boldsymbol{\theta}_2)\left(\boldsymbol{B}^H(\boldsymbol{\theta}_1, \boldsymbol{\theta}_2)\boldsymbol{B}(\boldsymbol{\theta}_1, \boldsymbol{\theta}_2)\right)^{-1} \boldsymbol{B}^H(\boldsymbol{\theta}_1, \boldsymbol{\theta}_2). \tag{37}$$

The structure of this estimator is similar to that of the deterministic signal maximum likelihood DOA estimator. Hence, the optimization methods developed for this problem, including the alternating projections [12] and the clustering methods [3] can be used.

With the estimated parameters at hand, we can use (16) to estimate the array manifold. First, we obtain an estimate $\tilde{\boldsymbol{w}}$ of $\hat{\boldsymbol{w}}$ by substituting the ρ's and the θ's into (13). We then get

$$\tilde{w}_l(k) = \frac{1}{\sqrt{N}} \sum_{i=1}^{r_l} \tilde{\rho}_{i,l} e^{-jk\tilde{\theta}_{i,l}}. \tag{38}$$

By substituting $\tilde{\boldsymbol{W}} = \text{diag}(\tilde{w}_l)$ into (14), we obtain

$$\tilde{\boldsymbol{A}}_l = \boldsymbol{F}\tilde{\boldsymbol{W}}_l \boldsymbol{F}^H \tag{39}$$

which when substituted into (16) yields

$$\begin{aligned}
\tilde{\boldsymbol{a}}_m &= \left(\tilde{\boldsymbol{A}}^H \tilde{\boldsymbol{A}}\right)^{-1} \tilde{\boldsymbol{A}}^H \boldsymbol{y}_m \\
&= \boldsymbol{F}\tilde{\boldsymbol{D}}\left(\tilde{\boldsymbol{W}}_1^H \check{\boldsymbol{y}}_{m,1} + \tilde{\boldsymbol{W}}_2^H \check{\boldsymbol{y}}_{m,2}\right)
\end{aligned} \tag{40}$$

where

$$\tilde{\boldsymbol{A}} = \begin{bmatrix} \tilde{\boldsymbol{A}}_1 \\ \tilde{\boldsymbol{A}}_2 \end{bmatrix}. \tag{41}$$

V. THE RELATION TO THE SIMO BLIND EQUALIZATION AND IDENTIFIABILITY RESULTS

In this section, we cast the calibration problem as the identification of a single input multiple output (SIMO) system. This will enable us to derive identifiability conditions, as well as present an alternative derivation of the LS estimator for reflections parameters.

First, note that we can rewrite (11) as

$$\boldsymbol{y}_{m,l} = \boldsymbol{h}_l * \boldsymbol{a}_m + \boldsymbol{n}_{m,l} \qquad l = 1, 2 \tag{42}$$

where

$$\boldsymbol{h}_l(k) = \begin{cases} \rho_{i,l}, & \text{if } \theta_{i,l} = \dfrac{2\pi(N-k)}{N} \\ 0, & \text{otherwise.} \end{cases} \tag{43}$$

That is, the measurements are just a spatially filtered version of the "signal" $\boldsymbol{a}_m$ by FIR filters with coefficients $\rho_{i,l}$ at $\theta_{i,l}$ and zeros otherwise. Our problem can now be stated as follows.

Given the output of two linear systems driven by the same signal, reconstruct the input signal.

The problem is in the form of blind identification. However, several differences between our problem and the conventional blind identification problem exist.

1) The signal is periodic with known period.
2) The measurements are taken along a single period.
3) We have several pairs of output signals: one for each element of the array.
4) The filters are sparse, i.e., most of the coefficients are zero.
5) The length of the filters may be the same as the number of samples.

We next develop the LS estimator as a natural variation on the method of [10] in the frequency domain.

Using the convolution theorem (remembering that our signal is periodic), we obtain

$$\hat{\boldsymbol{y}}_{m,l} = \hat{\boldsymbol{h}}_l \circ \hat{\boldsymbol{a}}_m \tag{44}$$

where $\circ$ denotes element-wise multiplication. Hence

$$\hat{\boldsymbol{y}}_{m,1} \circ \hat{\boldsymbol{h}}_2 = \hat{\boldsymbol{y}}_{m,2} \circ \hat{\boldsymbol{h}}_1. \tag{45}$$

After some algebraic manipulations, using the relation between $\boldsymbol{w}$ and $\boldsymbol{h}$, we obtain the noiseless version of (24).

The fact that our LS estimator can be derived using the approach of [10] enables us to give a sufficient condition for identifiability. This condition is obtained by translating the sufficient condition for identifiability of [10]. However, since our channel is sparse, we will be able to obtain stronger identifiability conditions.

To that end, note that the problem is identifiable for channels with signature (r_1, r_2) (i.e., has a unique solution with at most r_1 reflections in the first set of measurements, and, at most, r_2 reflections in the second set in the noiseless case) if (32) has a unique solution with the true $(\boldsymbol{\theta}_1, \boldsymbol{\theta}_2)$ while having no solution with any other substitution of $\boldsymbol{\theta}_1', \boldsymbol{\theta}_2'$. For this condition to hold, it is sufficient and necessary that for any pair $(\boldsymbol{\theta}_1, \boldsymbol{\theta}_2)$ where $\boldsymbol{\theta}_1 \in \mathbb{C}^{2r_1}$ and $\boldsymbol{\theta}_2 \in \mathbb{C}^{2r_2}$, the matrix $\boldsymbol{B}(\boldsymbol{\theta}_1, \boldsymbol{\theta}_2)$ has full column rank. We shall elaborate on this to obtain some further conditions, which will be easier to verify. To simplify notation, we

will work with a single matrix B_k instead of with the full matrix B. The generalization is straightforward though notationally complex.

Let

$$\Lambda_l = \begin{bmatrix} \check{y}_{m,l}(0) & & \\ & \ddots & \\ & & \check{y}_{m,l}(N-1) \end{bmatrix} \quad (46)$$

and (47), shown at the bottom of the next page. Note that

$$B_m(\boldsymbol{\theta}_1, \boldsymbol{\theta}_2) = [\Lambda_1 \Lambda_2] C(\boldsymbol{\theta}_1, \boldsymbol{\theta}_2). \quad (48)$$

The second matrix is always full column rank due to the Vandermonde structure of each block. Thus, the identifiability condition boils down to having the first matrix preserve the column rank. Similar to the condition in [10], we can now split this condition into two conditions. The first demanding informative array manifold, and the second is a condition on identifiable channels. Factoring Λ_l similarly to (7), we obtain

$$\Lambda_l = \begin{bmatrix} \check{a}_m(0) & & \\ & \ddots & \\ & & \check{a}_{m,l}(N-1) \end{bmatrix}$$
$$\cdot \begin{bmatrix} \hat{w}_m(0) & & \\ & \ddots & \\ & & \hat{w}_{m,l}(N-1) \end{bmatrix}. \quad (49)$$

Thus, the following immediately follows.

Theorem 5.1: Let $L = 2(r_1 + r_2 - 1)$. Assume that for every $0 \le k \le L - 1$, $\check{a}_m(k) \ne 0$ and $\hat{w}_1(k)$ and $\hat{w}_2(k)$ are not simultaneously zero; then, there is a unique solution to the problem (30).

Note that our conditions depend on the number of reflections rather than the channel length. We can, of course, weaken the condition above. However, the above condition for the array manifold typically holds, leaving us with conditions on the channels that hold, e.g., if the channel polynomials do not have common zeros on the unit circle.

VI. SIMULATION RESULTS

In this section, we present the results of several simulated experiments that demonstrate the performance of the algorithm. In all experiments, the array consisted of two sensors that were 2.5λ apart , and the number of reflections was 2, i.e., $r_1 = r_2 = 2$.

In the first experiment, the directions of the signals were $\theta_{1,1} = \theta_{1,2} = 0°$, and those of the multipath were
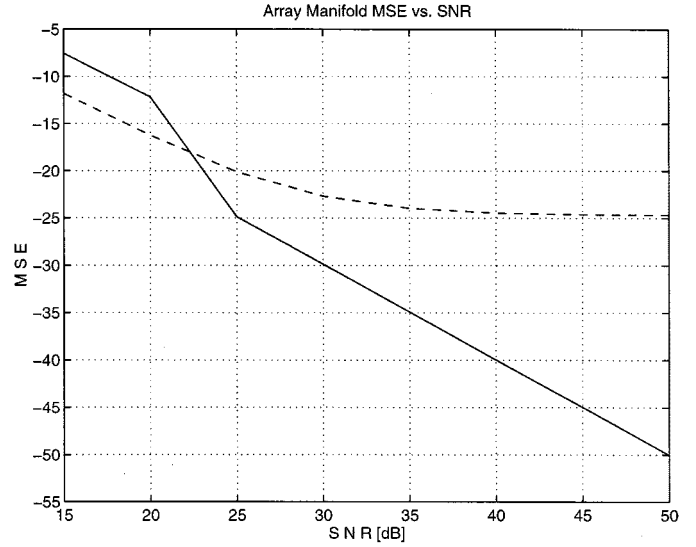

Fig. 2. Array manifold errors versus SNR. Multipath conditions: $\rho_{1,1} = 1$, $\rho_{1,2} = 0.03 + 0.05j$, $\rho_{2,1} = 1$, $\rho_{2,2} = 0.13 + 0.19j$. $\theta_{11} = \theta_{21} = 0°$, $\theta_{12} = 15°$, $\theta_{22} = 40°$. $S/M_1 = 25$ dB, $S/M_2 = 13$ dB. Solid line: error after application of the algorithm. Dashed line: error due to multipath (first set of measurements).

$\theta_{1,2} = 15°, \theta_{2,2} = 40°$ (Note that this does not limit the generality of the simulations since, as explained earlier, we can align the direct paths of the two measurements and only estimate the angles of the multipaths relative to the direct path. Typically, after alignment, the multipath will arrive with different AOA's, due to the fixed geometry of the reflectors.) The reflection coefficients were $\rho_{1,1} = \rho_{1,2} = 1$, $\rho_{1,2} = 0.03 + 0.05j$, $\rho_{2,2} = 0.13 + 0.19j$, which corresponds to signal to multipath ratios of 25 and 13 dB, respectively. At each SNR, we have performed 25 Monte Carlo trials. Fig. 2 shows the array manifold error averaged over all DOA's as a function of the SNR. While the solid line represents the error after application of the algorithm, the dashed line presents the array manifold error in the first set of measurements. The array manifold estimation MSE is computed by

$$\text{MSE} = \frac{1}{NM} \sum_{m=1}^{M} \sum_{k=1}^{N} \left\| \hat{a}\left(\frac{2\pi k}{N}, m\right) - a\left(\frac{2\pi k}{N}\right) \right\|^2 \quad (50)$$

where M is the number of trials, and N is the grid size. In all experiments, $M = 25$, $N = 360$, and $\hat{a}(2\pi k/N, m)$ is the mth estimate of $a(2\pi k/N)$. To gain further insight into the performance of the algorithm, we present in Fig. 3 the results of a

$$C(\boldsymbol{\theta}_1, \boldsymbol{\theta}_2) = \begin{bmatrix} \begin{array}{ccc} e^{-j0\theta_{21}} & \cdots & e^{-j0\theta_{2r_1,1}} \\ \vdots & & \vdots \\ e^{-j(N-1)\theta_{11}} & \cdots & e^{-j(N-1)\theta_{2r_1,1}} \end{array} & \mathbf{0} \\ \mathbf{0} & \begin{array}{ccc} e^{-j0\theta_{12}} & \cdots & e^{-j0\theta_{2r_2,2}} \\ \vdots & & \vdots \\ e^{-j(N-1)\theta_{12}} & \cdots & e^{-j(N-1)\theta_{2r_2,2}} \end{array} \end{bmatrix} \quad (47)$$
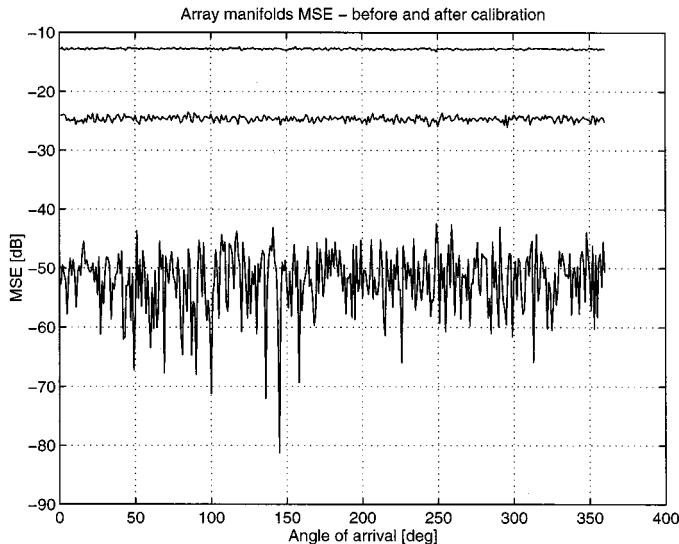
Fig. 3. Array manifold errors versus DOA. Multipath conditions: $\rho_{1,1} = 1$, $\rho_{1,2} = 0.03 + 0.05j$, $\rho_{2,1} = 1$, $\rho_{2,2} = 0.13 + 0.19j$. $\theta_{11} = \theta_{21} = 0°$, $\theta_{12} = 15°$, $\theta_{22} = 40°$. $S/M_1 = 24$ dB, $S/M_2 = 13$ dB. Bottom line: error after application of the algorithm. Upper lines: Error due to multipath (in two sets of measurements).
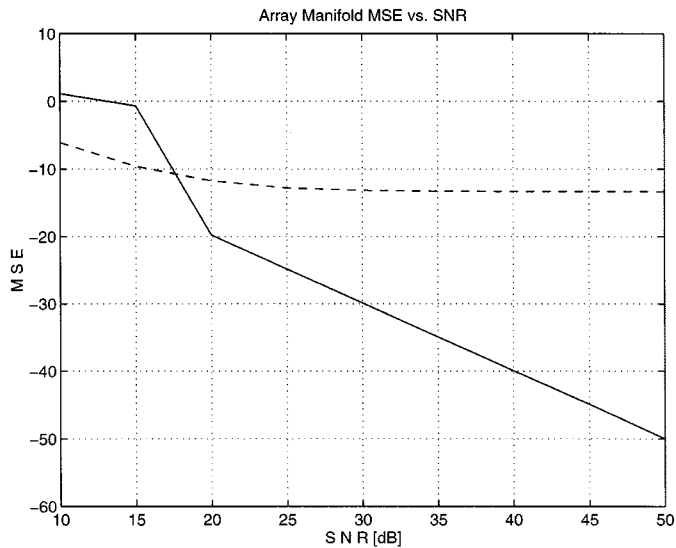

Fig. 4. Array manifold errors versus SNR. Multipath conditions: $\rho_{1,1} = 1$, $\rho_{1,2} = 0.21 + 0.05j$, $\rho_{2,1} = 1$, $\rho_{2,2} = 0.13 + 0.19j$. $\theta_{11} = \theta_{21} = 0°$, $\theta_{12} = 15°$, $\theta_{22} = 25°$. $S/M_1 = 13$ dB. $S/M_2 = 12$ dB. Solid line: error after application of the algorithm. Dashed line: error due to multipath (first set of measurements).

single experiment performed at SNR of 50 dB. We can see that the error after the application of the algorithm is much smaller than the error at the raw set of measurements. Moreover we see that the error is about the same for all DOA's.

In the second experiment, the directions of the signals were $\theta_{1,1} = \theta_{1,2} = 0°$, and those of the multipath were $\theta_{1,2} = 15°$, $\theta_{2,2} = 25°$. The reflection coefficients were $\rho_{1,1} = \rho_{1,2} = 1$, $\rho_{1,2} = 0.21 + 0.05j$, $\rho_{2,2} = 0.13 + 0.19j$ corresponding to signal to multipath ratios of 13 and 12 dB. At each SNR, we have performed 25 trials. Fig. 4 shows the array manifold error averaged over all DOA's as a function of the SNR. Whereas the solid line represents the error after
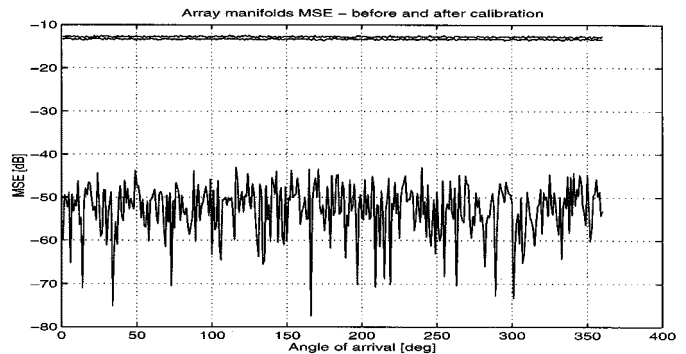

Fig. 5. Array manifold errors versus DOA. Multipath conditions: $\rho_{1,1} = 1$, $\rho_{1,2} = 0.21 + 0.05j$, $\rho_{2,1} = 1$, $\rho_{2,2} = 0.13 + 0.19j$. $\theta_{11} = \theta_{21} = 0°$, $\theta_{12} = 15°$, $\theta_{22} = 25°$. $S/M_1 = 13$ dB. $S/M_2 = 12$ dB. Bottom line: error after application of the algorithm. Upper lines: error due to multipath (in two sets of measurements).
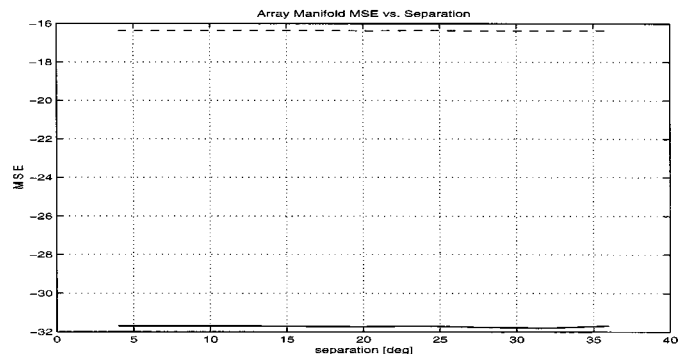

Fig. 6. Error as a function of $\theta_{22} - \Delta\theta_{12}$. Multipath conditions: $\rho_{1,1} = 1$, $\rho_{1,2} = 0.11 + 0.2j$, $\rho_{2,1} = 0.7$, $\rho_{2,2} = 0.055 + 0.2j$. SNR $= 30$ dB. Dashed line: the error due to the multipath. Solid line: the error after the application of the algorithm.

application of the algorithm, the dashed line presents the array manifold error in the first set of measurements. Fig. 5 shows the results of a single experiment performed at SNR of 50 dB. We can see that the error after the application of the algorithm is much smaller than the error at the raw set of measurements. Moreover, we see that the error is about the same for all DOA's.

In these two experiments, we clearly see that the improvement is not only obvious, but the error reduces to the level of the measurement noise. This demonstrates that the multipath is completely removed.

In the third experiment, the relative angular separation between the reflections in the first set of measurements was held fixed at 15°, whereas the relative angular separation in the second set of measurements varied from 19–51° in steps of 4°. The reflection coefficients were $\rho_{1,1} = 1$, $\rho_{1,2} = 0.11 + 0.1j$, $\rho_{2,1} = 0.7$, and $\rho_{2,2} = 0.055 + 0.2j$, and the SNR was 30 dB. The results are presented in Fig. 6. Notice that the performance of the algorithm is essentially independent of the angular separation.

VII. CONCLUDING REMARKS

We have presented a novel method for the calibration of sensor arrays in the presence of multipath. The method is based on measuring the array manifold from two angularly separated

locations and involves a solution of a multidimensional optimization. The method does not depend on the relative angular locations of the reflections.

ACKNOWLEDGMENT

REFERENCES

[1] J. Capon, "High resolution frequency-wavenumber spectrum analysis," *Proc. IEEE*, pp. 1408–1418, 1969.
[2] P. J. Davis, *Circulant Matrices*, New York: Wiley, 1979.
[3] A. Leshem and A. Y. Kasher, "Maximum likelihood direction finding using clustering methods," in *Proc. ICSP*, Beijing, China, 1993, pp. 1210–1214.
[4] R. O. Schmidt, "A signal subspace approach to multiple emmiter location and spectral estimation," Ph.D. dissertation, Stanford Univ., Stanford, CA, 1981.
[5] C. M. S. See, "Method for array calibration in high resolution sensor array processing," *Proc. Inst. Elect. Eng.—Radar, Sonar, Navig.*, pp. 90–96, June 1995.
[6] A. Swindlehurst and T. Kailath, "A performance analysis of subspace-based methods in the presence of model errors—Part 1: The music algorithm," *IEEE Trans. Signal Processing*, vol. 40, pp. 1758–1774, July 1992.
[7] ——, "A performance analysis of subspace-based methods in the presence of model errors—Part 2: Multidimensional algorithms," *IEEE Trans. Signal Processing*, vol. 41, pp. 2882–2890, Sept. 1993.
[8] M. Viberg and B. Ottersten, "Sensor array processing based on subspace fitting," *IEEE Trans. Acoust., Speech, Signal Processing*, vol. 39, pp. 1110–1121, May 1991.
[9] A. J. Weiss and B. Friedlander, "Array shape calibration using sources in unknown locations—A maximum likelihood approach," *IEEE Trans. Acoust., Speech, Signal Processing*, vol. 37, pp. 1958–1966, Dec. 1989.
[10] G. Xu, H. Liu, L. Tong, and T. Kailath, "A least squares approach to blind channel identification," *IEEE Trans. Signal Processing*, vol. 43, pp. 2982–2993, Dec. 1995.
[11] J. Yang and A. Swindlehurst, "The effects of array calibration errors on DF-based signal copy performance," *IEEE Trans. Signal Processing*, vol. 43, pp. 2724–2732, Nov. 1995.
[12] I. Ziskind and M. Wax, "Maximum likelihood localization of multiple sources by alternating projections," *IEEE Trans. Acoust., Speech, Signal Processing*, vol. 36, pp. 1553–1560, Oct. 1988.

Amir Leshem (M'98) received the B.Sc. degree (cum laude) in mathematics and physics, the M.Sc. degree (cum laude) in mathematics, and the Ph.D. degree in mathematics, all from the Hebrew University of Jerusalem, Jerusalem, Israel, in 1986, 1990, and 1997, respectively.

From 1984 to 1991, he served in the Israeli Defence Forces. From 1990 to 1997, he was a Researcher with the RAFAEL Signal Processing Center. From 1992 to 1997, he was also a Teaching Assistant with the Institute of Mathematics, Hebrew University of Jerusalem. Since 1998, he has been with the Faculty of Information Technology and Systems, Delft University of Technology, Delft, The Netherlands, working on algorithms for the reduction of electromagnetic interference in radio-astronomical observations and signal processing for communication. His main research interests include array and statistical signal processing, radio-astronomical imaging methods, set theory, logic, and foundations of mathematics.

Mati Wax (S'81–M'81–SM'88–F'94) received the B.Sc. and M.Sc. degrees from the Technion, Haifa, Israel, in 1969 and 1975, respectively, and the Ph.D. degree from Stanford University, Stanford, CA, in 1985, all in electrical engineering.

From 1969 to 1973, he served as an Electronic Engineer with the Israeli Defence Forces. In 1974, he was with A.E.L., Israel. In 1975, he joined RAFAEL, Haifa, where he headed the center for signal processing. In 1984, he was a Visiting Scientist at IBM Almaden Research Center, San Jose, CA. His research interests are in array signal processing and statistical modeling. Since 1997, he has been with U.S. Wireless Corporation, San Ramon, CA.

Dr. Wax was the recipient of the 1985 Senior Paper Award of the IEEE Acoustic, Speech, and Signal Processing Society.